

## Seismic Interaction between Pairs of Adjacent Structures and Implications for Performance-Based Earthquake Engineering

J.A. Knappett<sup>1</sup>, P. Madden<sup>2</sup>, K. Caucis<sup>3</sup>, Y. Gu<sup>4</sup>

### ABSTRACT

Widespread damage within urban centres (e.g. in the 2011 Christchurch Earthquake) has highlighted the need to better understand the seismic structure-soil-structure interaction (SSSI) between closely-spaced adjacent building structures. In this paper, such interaction will firstly be investigated for one single and two identical adjacent model building structures on non-liquefiable soil, using a combination of dynamic centrifuge modelling and non-linear elasto-plastic Finite Element (FE) modelling. After validating the FE approach against the centrifuge test data, it is subsequently used within a Monte-Carlo approach to simulate response under a range of 20 different input motions of differing spectral characteristics, at a range of shaking strengths. This will demonstrate the sensitivity of the observed SSSI behaviour to the input motion characteristics. Finally, this set of results will be interpreted in a probabilistic sense to demonstrate how the effects of SSSI may be incorporated within a Performance-Based Earthquake Engineering framework.

### Introduction

Despite recent advances in understanding seismic soil-structure interaction over the last 50 years, comparatively little is known about the structure-soil-structure interaction (SSSI) that will occur between adjacent structures during earthquakes. The effects of SSSI may be detrimental on structural response compared to the conventional case of an isolated structure, or they may have a beneficial, protective effect. If the former is true, it is important to be able to quantify such effects to better understand the risk posed to structures in urban areas and be able to mitigate this. If the latter is true, there may be as yet unexplored avenues in seismically resilient design to be discovered, where the grouping and relative dynamic properties of adjacent structures may be selected to obtain maximum benefit from the SSSI. In this paper the effect of an adjacent identical structure will be investigated using centrifuge modelling to validate numerical Finite Element Modelling (FEM), before this is subsequently used to undertake Monte-Carlo simulations and provide insight into the potential effects of SSSI on the seismic response of a structure and its foundations.

### Centrifuge Modelling

The results of two centrifuge tests are reported here – test PM004 considered a single, isolated structure, while test PM006 considered two adjacent structures, each identical to that used in

---

<sup>1</sup>Senior Lecturer, Div. of Civil Engineering, University of Dundee, Dundee, UK, [j.a.knappett@dundee.ac.uk](mailto:j.a.knappett@dundee.ac.uk)

<sup>2</sup>PhD student, Div. of Civil Engineering, University of Dundee, Dundee, UK, [p.madden@dundee.ac.uk](mailto:p.madden@dundee.ac.uk)

<sup>3</sup>Graduate Engineer, Arup, Edinburgh, UK, [karlis.caucis@arup.com](mailto:karlis.caucis@arup.com) (formerly University of Dundee)

<sup>4</sup>MSc student, Div. of Civil Engineering, University of Dundee, Dundee, UK, [y.gu@dundee.ac.uk](mailto:y.gu@dundee.ac.uk)

PM004, with 1 m of clear space between the edges of the foundations of the adjacent structures. This section will describe the modelling procedures; results are summarised later in direct comparison to the FEM. In each case the subsoil profile and sequence of input motions were kept the same. Both tests were conducted at 1:50 scale at 50-g using the Actidyn C67-2 3.5 m radius beam centrifuge at University of Dundee, UK. All subsequent parameters and results are given at prototype scale, unless otherwise stated. Figure 1 shows the layout of test PM006 as an example.

The structural model in each case was modelled as a single bay, single-degree-of-freedom (SDOF) sway frame on separated strip foundations, 5 m long  $\times$  2 m wide at prototype scale (100 mm  $\times$  40 mm at model scale). Steel mass plates were used to represent the dynamic mass of the structure, which were located 7.5 m above the founding plane (i.e. the structure was 150 mm tall to the centre of mass). Vertical aluminium alloy plates, the same length as the foundations, were used to represent the sway stiffness of the structures that would be provided by the columns. The mass of the steel plates and bending stiffness of the aluminium plates were set such that the fixed-base natural period of the structure was 0.65 s and the bearing pressure was 276 kPa. It can be seen from Figure 1 that the structures occupied a maximum of the central 33% of the model container to minimise any potential boundary effects.

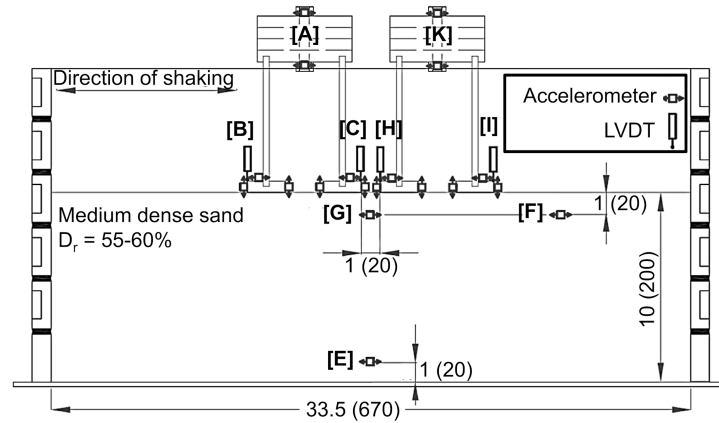


Figure 1. Centrifuge model layout for test PM006, dimensions in m at prototype scale (model scale in mm)

The subsoil profile consisted of 10 m of dry (i.e. non-liquefiable) silica sand (Congleton HST95) prepared to a uniform relative density of 59% in PM004 and 58% in PM006. This was pluviated in air into an Equivalent Shear Beam (ESB) container, the design and performance of which is described in Bertalot (2012). The sand had  $G_s = 2.63$ ,  $D_{10} = 0.09$  mm,  $e_{\max} = 0.769$  and  $e_{\min} = 0.467$ . For these soil conditions (resulting in unit weight  $\gamma = 16.2$  kN/m<sup>3</sup> and peak friction angle  $\phi'_p = 40^\circ$ ), the static vertical factor of safety of the foundations was estimated as 5.5, after Lyamin et al. (2007).

Following spin-up of the centrifuge to 50-g, the initial settlement and tilt of the model structures were firstly recorded before a sequence of strong ground motions was applied using the Actidyn QS67-2 servo-hydraulic earthquake simulator (EQS), the performance of which is detailed in Brennan et al. (2014). Each model was subjected to an extensive sequence of input motions of

varying strength, but only the results of the first two motions are reported here. In each case a horizontal motion recorded at the Nishi-Akashi recording station in the  $M_w = 6.9$  Kobe earthquake (1995) was used. This record was downloaded from the PEER (Pacific Earthquake Engineering Research) NGA database and was (i) rescaled to a peak acceleration of  $a_g = 0.1\text{-g}$  in the first motion and  $0.5\text{-g}$  in the second; and (ii) band-pass filtered between  $0.8\text{ Hz}$  and  $8\text{ Hz}$  ( $40\text{--}400\text{ Hz}$  at model scale) using a zero-phase-shift digital filter to remove components of the signal that were outside the range that can be accurately controlled by the EQS. The time history of the motion input to EQS, normalised by peak acceleration, is shown in Figure 2, along with elastic response spectra of all motions as recorded at location [E] in the tests (see Figure 1) for nominal 5% structural damping.

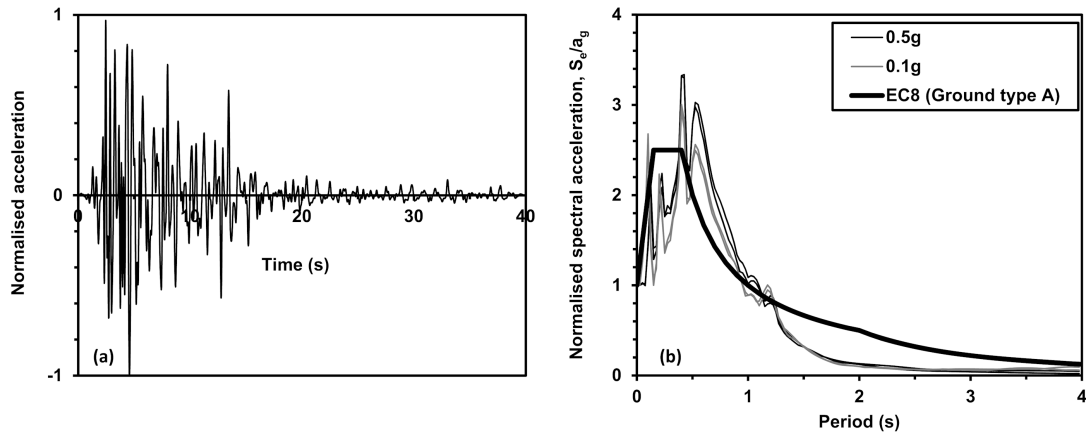


Figure 2. Input motion, normalized by peak acceleration: (a) time history; (b) response spectrum.

### Finite Element Modelling (FEM)

As the centrifuge model structures and foundations were long in the direction perpendicular to shaking, finite element simulations of all of the tests were conducted in plane strain using PLAXIS 2D 2012. The dimensions of the model domain were extended laterally to  $100\text{ m}$  and combined with non-reflecting boundary elements controlling the dynamic stresses along the vertical boundaries (after Lysmer and Kuhlmeyer, 1969) to represent semi-infinite soil conditions, i.e. boundary deformations at the location of the centrifuge container wall which were controlled by the dynamic deformation of the adjacent soil. Figure 3 shows the FEM layout and mesh for test PM006 (for direct comparison with Figure 1). The hatching at the bottom of Figure 3 are actually a series of arrows representing the input motion.

The soil was modelled using the ‘Hardening Soil model with small-strain stiffness’ (Benz, 2006). This model incorporates non-linear elastic behaviour which is dependent on both confining stress level and induced strain, with Mohr-Coulomb plasticity having isotropic hardening. Full details of the soil parameter correlations used may be found in Knappett et al. (2015) and the calibration of these correlations for the HST95 sand used are presented in Al-Defae et al. (2013). A more detailed discussion of the influence of using different soil parameter sets across a wider database of centrifuge tests for SSSI problems may be found in Knappett et al. (2015). The equivalent mass and vertical plates of the structures were modelled numerically using elastic plate elements

having the same bending stiffness per metre length ( $EI = 155.1 \text{ MNm}^2/\text{m}$  for each vertical plate) and mass (469 t for all mass plates combined) as the centrifuge models. The footings were modelled as an elastic continuum with Young's modulus of 210 GPa, Poisson's ratio of 0.3 and unit weight of  $76.5 \text{ kN/m}^3$  to match the properties of the steel footings in the centrifuge tests. Equivalent viscous damping ( $\zeta$ ) within the structure was modelled using Rayleigh's approach

$$\zeta = c_m \left( \frac{1}{4\pi f_n} \right) + c_k (\pi f_n) \quad (1)$$

where  $c_m = 0.4$  and  $c_k = 0.001$  were determined through fitting Equation 1 to measurements obtained from the results of impulse tests on the centrifuge model structures.

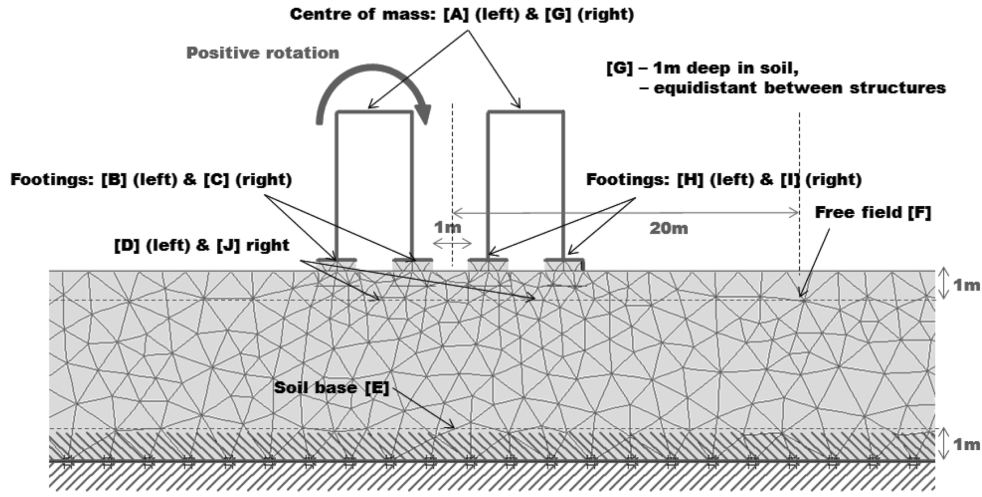


Figure 3. Example Finite Element model (near-field of test PM006 shown).

The initial conditions in each FEM simulation were obtained by initially generating a  $K_0$  stress condition in the soil (where  $K_0 = 1 - \sin \phi'_p$ ), followed by 'building' the structure(s) in a static stage where the weight of the structure(s) was applied to the soil resulting in some initial settlement and a very small non-zero tilt of the structure. At this stage, the initial conditions were 'ideal', but were not the same as those measured following spin-up in the centrifuge. Variation of the initial conditions was found to have a dramatic effect on the ability of the FEM to replicate the centrifuge observations, and so a further set of additional vertical point loads were applied to the foundation (points [B], [C], [H] and [I] in Figure 3) during the initial static step to generate a couple which forced the structure to have the initial rotations measured in the centrifuge tests. Such a couple, superimposed on the initially equally divided vertical loads, simulated the load distribution between footings that was consistent with the measured structural rotation, without changing the net bearing pressure. The magnitude and direction of the couple in each case were determined by trial and error within the initial static step of the corresponding FE model to match the resulting rotations to those measured in the centrifuge tests. A more detailed discussion of the influence of the structural initial conditions on subsequent dynamic response across a wider database of centrifuge tests may be found in Knappett et al. (2015). Once representative initial conditions had been achieved, a final dynamic stage was applied to

the model in which dynamic ground displacement time histories (as measured during the corresponding centrifuge test) were applied to the bottom of the soil model, with all analysis being conducted in the time domain.

### Validation of FEM

Figure 4 shows a comparison of some key measures of model performance. The first parameter shown is free-field site amplification (Figure 4a), namely the peak acceleration at point [F] divided by the peak input acceleration as measured at point [E]. This is included to verify that the transmission of the earthquake motion towards the structure is correctly captured (i.e. that the soil constitutive model is appropriate for simulating the dynamic response of the soil). There is a slight under-prediction of the amplification in the larger motions for these particular cases (simulations against further centrifuge tests with the same soil that can be found in Knappett et al., 2015 were better), but the numerical model correctly captures the high amplification in the small motions (0.1-g) and the significant reduction in amplification in the larger motion, due to the increasingly plastic soil response.

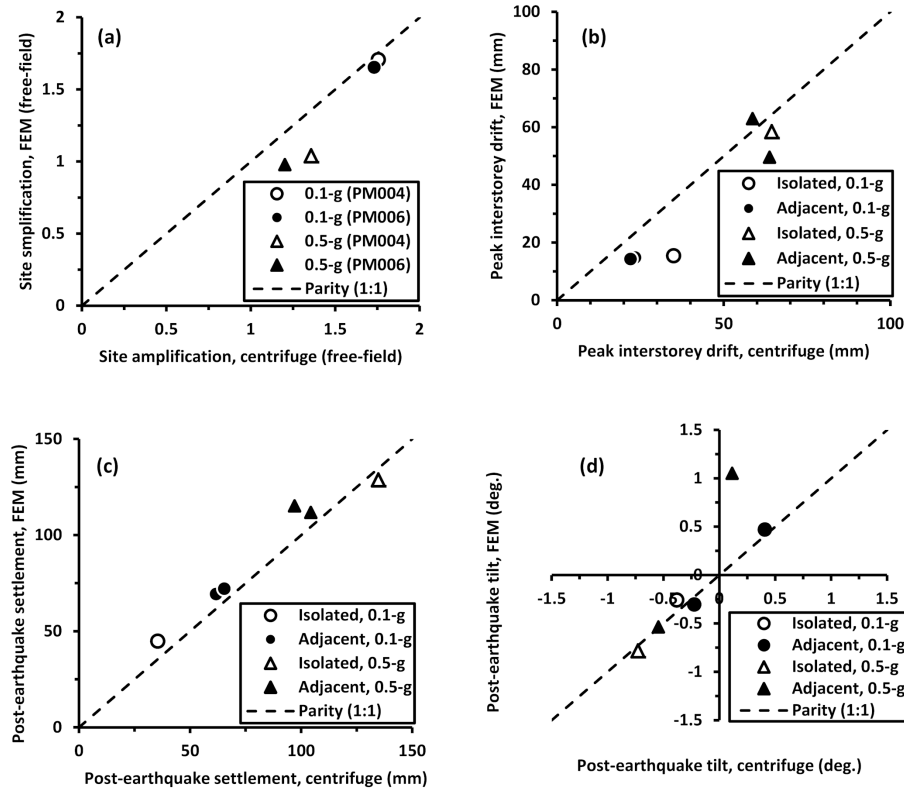


Figure 4. Validation of FEM against centrifuge test data: (a) site amplification factor; (b) peak elastic interstorey drift; (c) post-earthquake settlement; (d) post-earthquake structural tilt.

The soil-structure interaction is represented by the peak elastic interstorey drift (Figure 4b), post-earthquake average settlement (Figure 4c) and overall tilt (Figure 4d) of the structures. These parameters are generally replicated very well, both for isolated and adjacent structure cases. The

FEM predicted similar increases in interstorey drift during stronger earthquakes, though it should be noted that there appears to be little effect of structure-soil-structure interaction on this parameter in this particular case. The FEM also correctly predicts the reduced amount of settlement occurring as a result of the second, stronger earthquake in the adjacent case (compare 0.1-g and 0.5-g filled points in Figure 4c) compared to the isolated structure case (compare similar hollow markers in Figure 4c). Considering the overall post-earthquake structural tilt (Figure 4d), the FEM does an admirable job, with the exception of a single datapoint for the 0.5-g adjacent case. This has occurred because the rotational response of adjacent structures is highly sensitive to the initial tilt, such that any small variations in the first earthquake may be grossly exaggerated in subsequent earthquakes. A detailed discussion of this effect may be found in Knappett et al. (2015), where the divergence between measured and predicted values becomes highly prominent for subsequent motions beyond the first two. Therefore, in the following section, the effect of different input motions will be simulated in each case using the same ideal initial conditions for models which have not undergone any pre-shaking.

### Implications for Performance-Based Earthquake Engineering

Based on the results for the single motion considered in the centrifuge tests (Figure 2), Figure 4 suggested that there was a negligible effect of SSSI on drift and rotation and potentially a beneficial effect in reducing permanent settlement (at least in low intensity motions). In order to confirm whether this is a more general result, or a function of the specific motion used, the validated FE models of both the isolated and adjacent structure cases were subjected to a wider database of twenty ground motions from the PEER NGA database (recorded at locations where shear wave velocity > 600 m/s), each of which was normalised and rescaled to strengths of 0.1, 0.2, 0.3, 0.4 and 0.5-g. Normalised elastic response spectra for nominal 5% damping are shown in Figure 5.

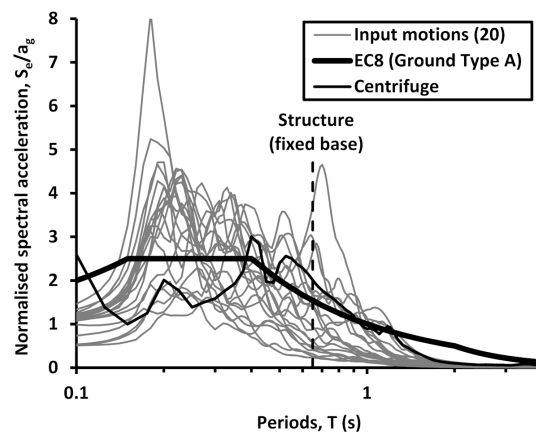


Figure 5. Elastic response spectra used in parametric study (nominal 5% damping).

The result of the one hundred isolated and adjacent structure simulations, in terms of the peak interstorey drift, post-earthquake structural settlement and post-earthquake tilt are shown in Figures 6 to 8. Part (a) of each of these figures plots the data for each of the adjacent structures against the behaviour of the comparative isolated structure. To indicate what the implications for performance based design are in this case, a performance limit was set for each parameter

beyond which damage was expected (the ‘damage limit’). At each input strength, each of the twenty simulation results was compared to this limit to obtain the probability of exceeding the damage limit to the nearest 5%. The resulting data is shown in the part (b) of each figure, and represents the fragility curve for the particular suite of motions considered in this study.

From Figure 6a, it can be seen that there is a general increase in peak interstorey drift due to SSSI. The damage limit selected was  $1/300^{\text{th}}$  of the storey height, which might represent sufficient drift to damage any infill walls within the framed structure. This is expressed in Figure 6b in terms of an increase in the probability of exceedence by up to 15%. From Figure 7a, there is a general reduction in settlement due to SSSI. For a damage limit of post-earthquake settlement  $< 50$  mm there is up to 20% reduction in the probability of exceedence (Figure 7b). In terms of post-earthquake tilt, there is a substantial increase in the magnitude of rotation due to SSSI (Figure 8a). Considering a damage limit of  $1/50$  (1.15 degrees), the probability of exceedence is significantly increased in the stronger motions due to SSSI (Figure 8b). Although only the magnitude of the tilt is indicated, the increased rotation in adjacent structure cases was generally always outwards (i.e. with the structures rotating away from each other) due to the increased confinement to the subsoil when the structures rotate towards each other.

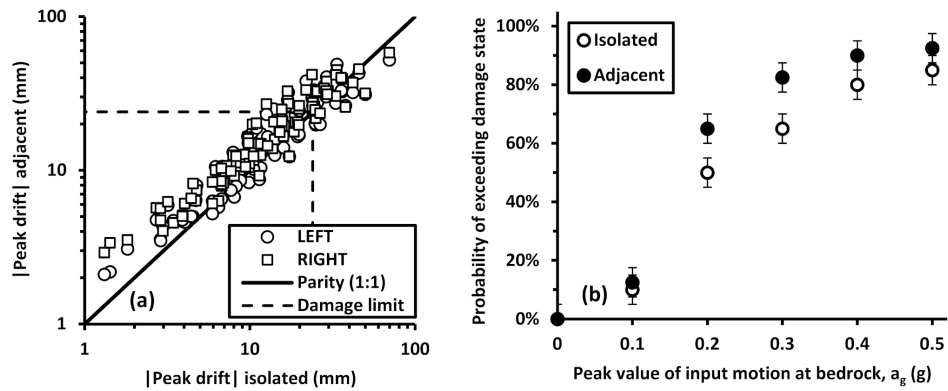


Figure 6. Peak interstorey drift from Monte-Carlo simulations: (a) data; (b) fragility curves.

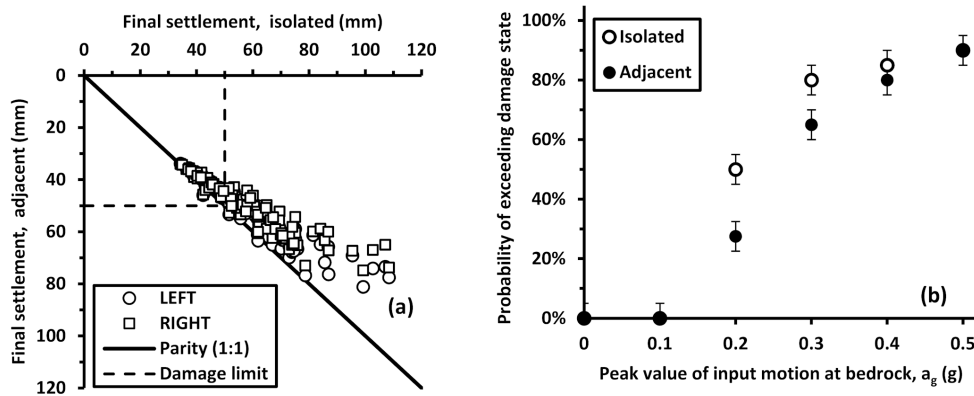


Figure 7. Post-earthquake settlement from Monte-Carlo simulations: (a) data; (b) fragility curves.

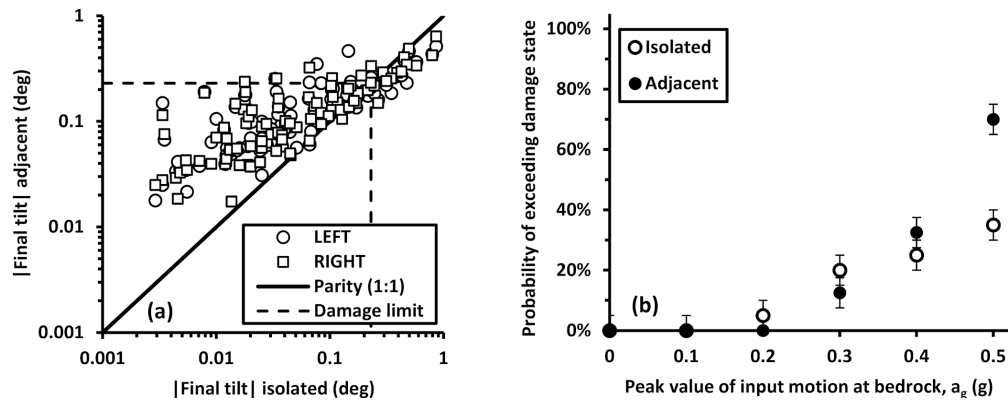


Figure 8. Post-earthquake tilt from Monte-Carlo simulations: (a) data; (b) fragility curves.

## Conclusions

Finite Element models of isolated and adjacent (paired) structures have been used to investigate seismic structure-soil-structure interaction for structures on non-liquefiable soil. The FE models were validated against dynamic centrifuge test data. Subsequently, Monte-Carlo simulations using the FE models demonstrated that for the particular case considered, SSSI was detrimental on peak interstorey drift (increasing the fragility curve by up to +15%), beneficial on post-earthquake settlement (up to -20%) and detrimental on post-earthquake tilt (substantial increases). The results suggest that with further research, it may be possible to account for SSSI through modifications to fragility curves for isolated structures.

## Acknowledgments

This work was supported by the Engineering and Physical Sciences Research Council (EPSRC) under Grant no. EP/H039716/1. The authors would also like to thank Mark Truswell and Colin Stark for their assistance in performing the centrifuge tests.

## References

- Al-Defae AH, Caucis K, Knappett JA. Aftershocks and the whole-life seismic performance of granular slopes. *Géotechnique* 2013; **63** (14): 1230-1244.
- Benz T. *Small-strain stiffness of soils and its numerical consequences*. PhD Thesis, U. of Stuttgart, Germany, 2006.
- Bertalot D. *Behaviour of shallow foundations on layered soil deposits containing loose saturated sands during earthquakes*. PhD Thesis, U. of Dundee, UK, 2012.
- Brennan AJ, Knappett JA, Bertalot D, Loli M, Anastasopoulos I, Brown MJ. Dynamic centrifuge modelling facilities at the University of Dundee and their application to studying seismic case histories. In: Gaudin C & White DJ (Eds.), *Proc. 8<sup>th</sup> Int. Conf. on Physical Modelling in Geotechnics*, 2014, Taylor & Francis: 227-233.
- Knappett JA, Madden P, Caucis K. Seismic structure-soil-structure interaction between pairs of adjacent building structures. *Géotechnique*, 2015 (In Press)
- Lyamin AV, Salgado R, Sloan SW, Prezzi M. Two- and three-dimensional bearing capacity of footings in sand. *Géotechnique*, 2007, **57** (8): 647-662.
- Lysmer J, Kuhlmeyer RL. Finite dynamic model for infinite media. *ASCE Journal of the Engineering Mechanics Division*, 1969, **95**: 859-887.